International journal of spray and combustion dynamics

International Journal of Spray and Combustion Dynamics
2018, Vol. 10(4) 393–398

DOI: 10.1177/1756827718819360
journals.sagepub.com/home/scd
SAGE

Corrigendum

Aswathy Surendran, Maria A Heckl, Naseh Hosseini, Omke Jan Teerling (2018). Passive control of instabilities in combustion systems with heat exchanger. International Journal of Spray and Combustion Dynamics, first published online October 13, 2017. (Original DOI: https://doi.org/10.1177/1756827717731486)

In the above-referenced article, the authors wish to make the following clarifications:

We have underestimated the passive control capability of heat exchangers (*hex*) due to an erroneous calculation of the 'heat sink coefficient' (α). Instead of using the *global* mean heat absorption rate at the hex ($\bar{Q}_h$) corresponding to the total cross-sectional area of the duct (S), we used the value for the absorption rate corresponding to the cross-sectional area of the domain shown in Fig. 3 of the original article. This error in the calculation caused us to neglect α (see Eq. (18)) in the parametric study and in the subsequent stability analysis.

Upon realising this error, we redid the analysis by rectifying the value for α. The latest results, though qualitatively similar from our previous conclusions, now present the following story. In this corrigendum, we have included only those sections from the original article that required revision/correction.

5 Parametric Study

From Sections 3 and 4, we can summarise that the overall scattering behaviour at the downstream end of the combustor will be dependent on the following physical processes

- vortex dissipation at the tube row (key parameter of interest is the mean flow velocity)
- trapping of acoustic waves in the cavity (key parameters of interest are the cavity length and the frequency)
- heat sink (or the heat absorption at the hex) acting as an acoustic sink/acoustic source depending on the system parameters (key parameters of interest are the mean flow velocity, the cavity length and the frequency)

Hence, to look at the influence of these physical processes on the scattering behaviour of the hex, we conduct parametric studies with respect to frequency (f), mean flow velocity ($\bar{u}$) and cavity length (l_c) for the cases with (a) tube row alone (only acoustic scattering and no heat absorption), (b) heat sink alone (only heat absorption and no tube row), and (c) hex with both acoustic scattering *and* heat absorption. The three different cases are considered to enable comparisons between the influences of acoustic scattering and heat sink processes occurring at hex as well as to identify the dominant process.

5.1 Influence of frequency (f)

The influence of frequency on $|R_L|$ and Δ_L are shown in Figures 7 and 8 respectively. Figures 7(a) and 8(a) show the behaviour of the cavity-backed tube row (without heat sink), while Figures 7(b) and 8(b) denote the behaviour for the heat sink (without tube row) and Figures 7(c) and 8(c) denote the behaviour for the hex with both tube row and heat sink, for $d = 3$ mm, $\eta = 0.1$, $l_c. = 0.25$ m and $\bar{u} = 0.5$, 1.0 and 1.5 m/s. In all the three cases and for the frequency range considered, it can be observed that with increasing f, $|R_L|$ decreases and f increases.

However, the variation of the curves with respect to the mean flow velocity show that for any given frequency, in the tube row only case, $|R_L|$ decreases with increasing velocity whereas Δ_L increases with increasing velocity. In the heat sink only case, we observe an opposite trend. Here, $|R_L|$ increases with increasing velocity and Δ_L decreases

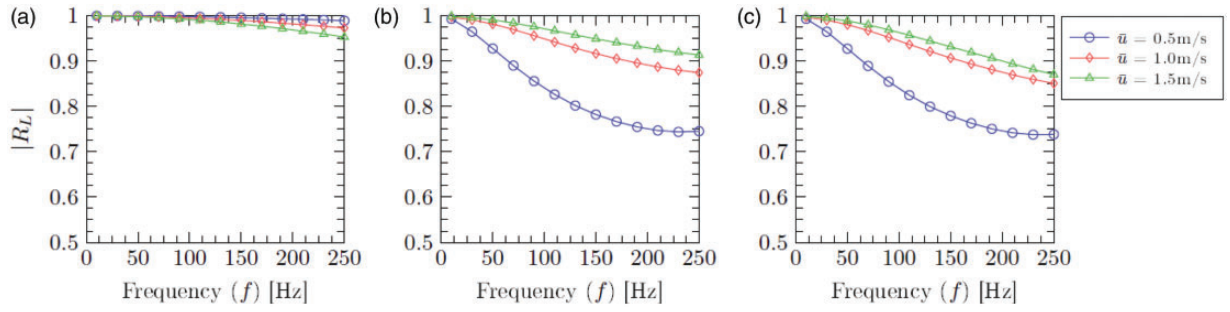

Figure 7. Variation of $|R_L|$with respect to frequency (f), for fixed velocities, $d = 3$ mm, $\eta = 0.1$ and $l_c = 0.25$ m. Subplots denote the behaviour for (a) tube row only, (b) heat sink only and (c) hex – combination of tube row and heat sink.

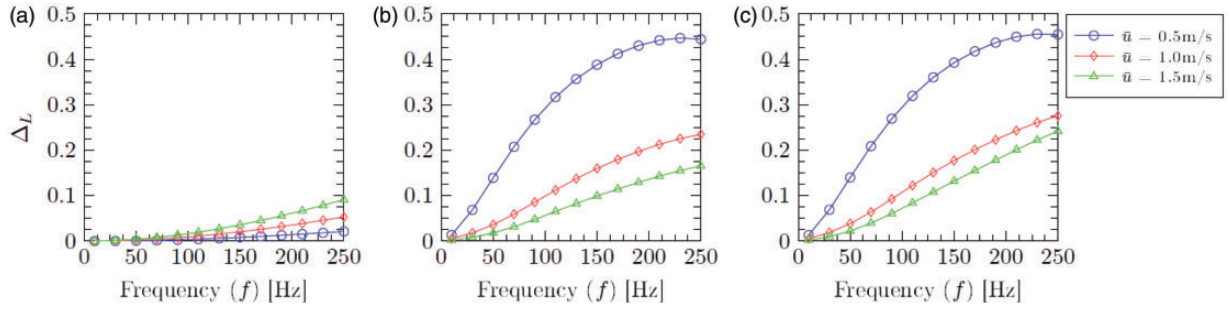

Figure 8. Variation of Δ_L with respect to frequency (f), for fixed velocities, $d = 3$ mm, $\eta = 0.1$ and $l_c = 0.25$ m. Subplots denote the behaviour for (a) tube row only, (b) heat sink only and (c) hex – combination of tube row and heat sink.

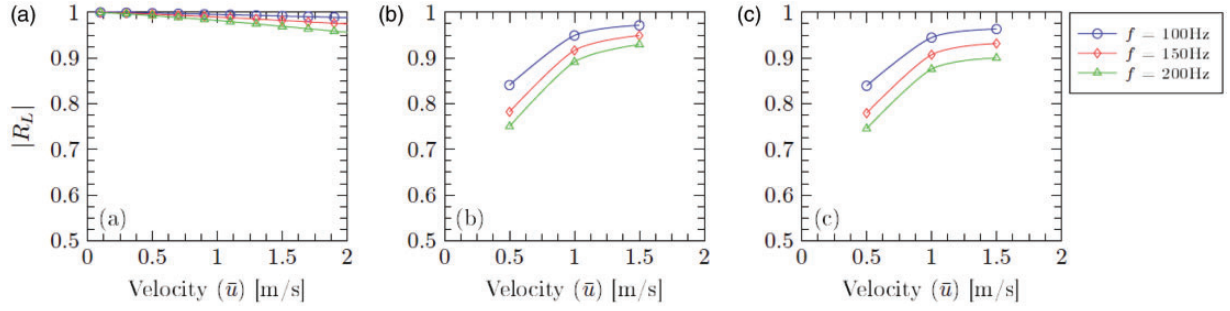

Figure 9. Variation of $|R_L|$ with respect to mean flow velocity ($\bar{u}$), for fixed frequencies, $d = 3$mm, $\eta = 0.1$ and $l_c = 0.25$ m. Subplots denote the behaviour for (a) tube row only, (b) heat sink only and (c) hex – combination of tube row and heat sink.

with increasing velocity. The behaviour of the hex will be a combination of the two processes: tube row and heat sink. From Figures 7(c) and 8(c), we can observe that the $|R_L|$ and Δ_L variations are close to those of the heat sink (Figures 7(b) and 8(b)) for low velocities and for increasing velocities, the influence is evidently a combination of both tube row and heat sink.

5.2 Influence of mean flow velocity ($\bar{u}$)

Figures 9 and 10 show the influence of the mean flow velocity ($\bar{u}$) on $|R_L|$ and Δ_L for three fixed frequencies: $f = 100$, 150 and 200 Hz, $d = 3$ mm, $\eta = 0.1$ and $l_c. = 0.25$ m. For the case with only tube row (Figures 9(a) and 10(a)) and for the velocity range considered, it can be observed that with increasing $\bar{u}$, $|R_L|$ decreases and Δ_L increases. This is due to the increased dissipation at the tube row due to vortex shedding. For the cases with heat

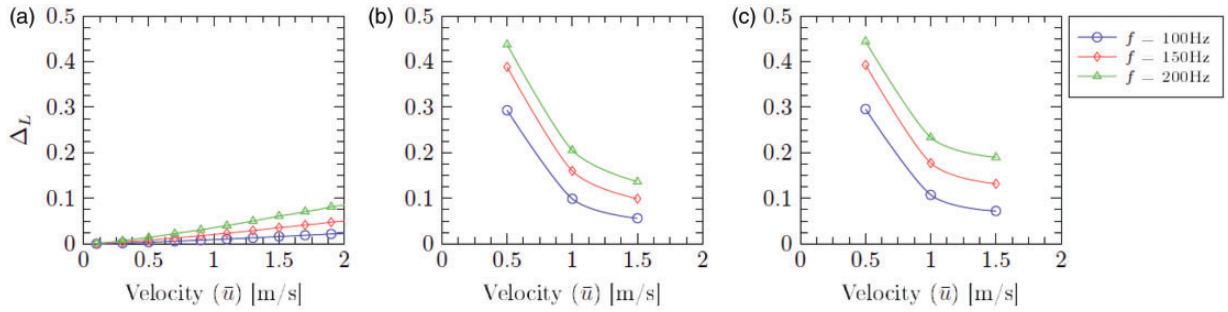

Figure 10. Variation of Δ_L with respect to mean flow velocity ($\bar{u}$), for fixed frequencies, $d = 3$ mm, $\eta = 0.1$ and $l_c = 0.25$ m. Subplots denote the behaviour for (a) tube row only, (b) heat sink only and (c) hex – combination of tube row and heat sink.

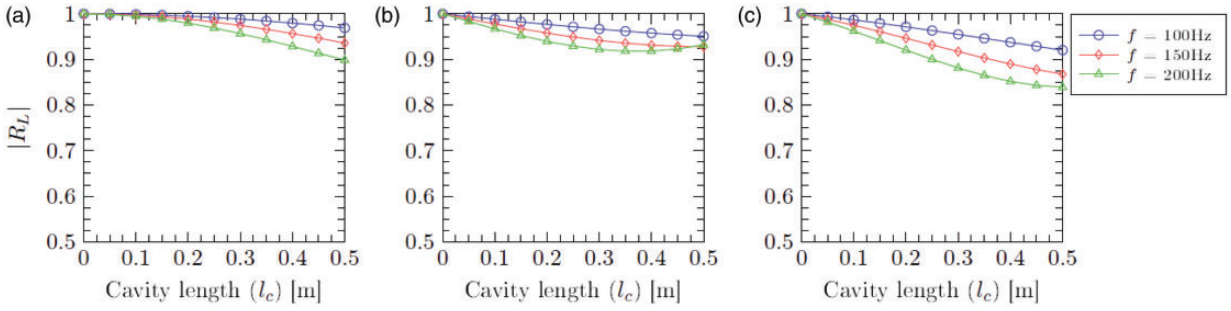

Figure 11. Variation of $|R_L|$ with respect to cavity length (l_c), for fixed frequencies, $d = 3$ mm, $\eta = 0.1$, $\bar{u} = 1.5$ m/s and $l_c = 0.25$ m. Subplots denote the behaviour for (a) tube row only, (b) heat sink only and (c) hex – combination of tube row and heat sink.

sink and hex, where heat absorption is significant, our analysis is restricted to only three velocities: $\bar{u} = 0.5$, 1.0 and 1.5 m/s owing to the availability of HTF simulation data for these velocities. In the case of the heat sink, it can be observed from Figures 9(b) and 10(b) that $|R_L|$ increases with increasing velocity, whereas Δ_L decreases with increasing $\bar{u}$. This behaviour may be attributed to the fact that with increasing velocity the net heat absorbed at the hex decreases, as is evidenced by the increase in the measured mean temperature downstream (refer to $\bar{T}_3$ provided in Table 1) of the hex with increasing $\bar{u}$.

The combined influence of the tube row and the heat sink is as shown in Figures 9(c) and 10(c), where $|R_L|$ increases with increasing velocity and Δ_L decreases with increasing $\bar{u}$. The plots depict that in our analysis, the influence of the heat sink dominates and the added influence of tube row is significant only for larger velocities like 1.5 m/s.

5.3 *Influence of cavity backing and resonance (l_c)*

Cavity backing can act as an additional resonator, causing resonance or anti-resonance depending on the downstream reflection coefficient R_p. In our analysis, $R_p = 1$ and the effect of the cavity length on the effective reflection and absorption coefficient of a cavity-backed tube row, heat sink and hex are shown in subplots (a), (b) and (c) respectively of Figures 11 and 12. For the case with only the tube row, we can observe that for the given cavity length range, $|R_L|$ decreases with l_c, whereas Δ_L increases with increasing l_c. If the range for the cavity length is increased further, it was observed that $|R_L|$ reaches a minimum and then increases, while Δ_L reaches a maximum and then decreases. This change in behaviour for $|R_L|$ (and Δ_L) is observed for that l_c value which is equal to the quarter wavelength of the incident frequency. Studies conducted on slit-plates backed by a rigid plate ($R_p = 1$) have shown that for an incident acoustic wave of frequency f, there will be maximum absorption if the cavity length is $l_c = c_4/(4f)$ [10], where c_4 is the speed of sound inside the cavity.

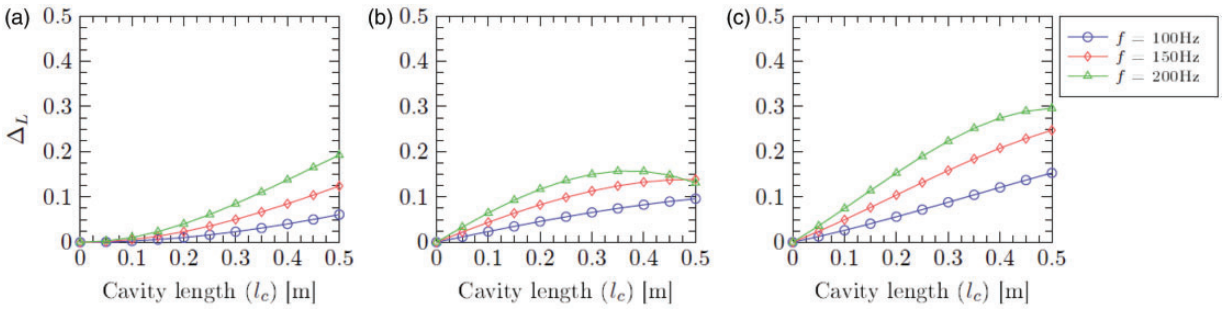

Figure 12. Variation of Δ_L with respect to cavity length (l_c), for fixed frequencies, $d = 3$ mm, $\eta = 0.1$, $\bar{u} = 1.5$ m/s and $l_c = 0.25$ m. Subplots denote the behaviour for (a) tube row only, (b) heat sink only and (c) hex – combination of tube row and heat sink.

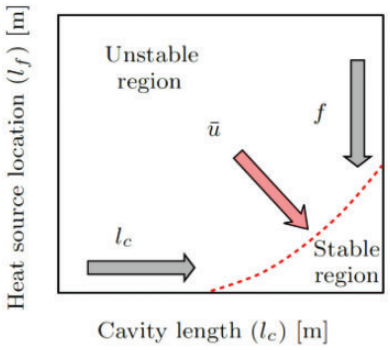

Figure 13 Expected trend for *decrease* in stability, as l_c, l_f and $\bar{u}$ vary.

For the cases with only the heat sink and the hex, though the variations of $|R_L|$ and Δ_L with increasing l_c are similar to those of the tube row, a relation between the incident frequency and the optimal value of l_c that produces maximum acoustic absorption cannot be formed, as a result of the influence of the heat sink i.e., in subplots (b) of Figures 11 and 12, the optimal l_c for $f = 200$ Hz is shown to be $\sim$0.35 m, whereas in subplots (c) it is $\sim$0.5 m.

6 Stability analysis of the combustor

6.3.3 *Influence of the mean flow velocity ($\bar{u}$)*

In Section 5.2, we have concluded that an increase in $\bar{u}$ decreases Δ_L, at least for the parameter range of interest in the present study. This decrease in Δ_L can be interpreted as the increase or the growth of the unstable region in the stability maps. This growth is indicated by the arrow along the diagonal in Figure 13.

Therefore, from the parametric study, we can expect that the hex, whose behaviour is a combination of the acoustic scattering at the tube row and the heat absorption at the heat sink, can stabilise an unstable mode of the combustor through the variation of parameters like frequency, mean velocity and cavity length. The stability maps constructed for the case with $d = 3$ mm, $\eta = 0.1$ and $\bar{u} = 0.5$, 1.0 and 1.5 m/s, shown in Figure 14, confirms our expected trend for instability growth. Also, there is a range of cavity lengths for a given $\bar{u}$ value where the system is stable irrespective of l_f. This stability and the range of l_c values can be improved further, by decreasing $\bar{u}$.

6.4 *Influence of heat loss and acoustic scattering on stability*

6.4.1 Influence of heat loss at hex. Except for the figure provided here, the explanation provided for this subsection in the original article remains unchanged.

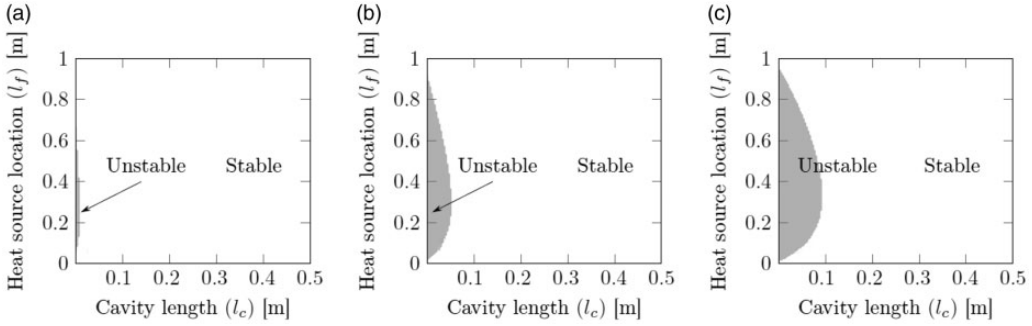

Figure 14 Stability maps obtained for $d = 3$ mm, $\eta = 0.1$ and incoming velocity of (a) $\bar{u} = 0.5$ m/s, (b) $\bar{u} = 1.0$ m/s and (c) $\bar{u} = 1.5$ m/s.

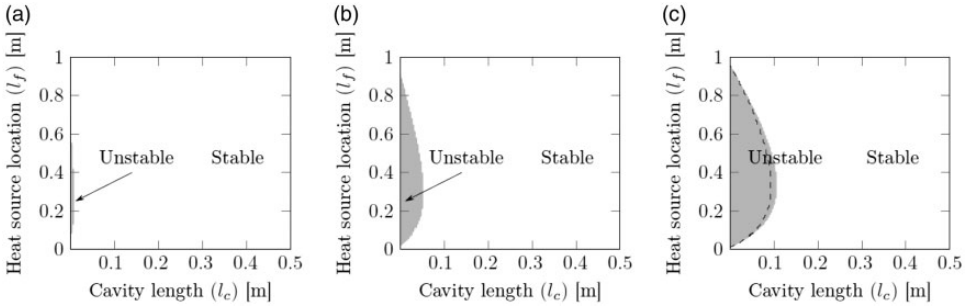

Figure 15 Stability maps obtained for $d = 3$ mm, $\eta = 0.1$ and incoming velocity of (a) $\bar{u} = 0.5$ m/s, (b) $\bar{u} = 1.0$ m/s and (c) $\bar{u} = 1.5$ m/s, in the presence of only the heat sink.

6.4.3 Influence of hex. The net influence of hex can now be treated as a combination of the influences of the heat sink and the acoustic scattering at the tube row. As $\bar{u}$ increases, the heat sink has a destabilising influence while the scattering at the tube row has a stabilising influence. Comparison of Figures 14 and 16 (in the original article) indicates that the influence of the heat sink determines the stability of the combustor. However, with increasing velocity, the stabilising effect of tube row will also become significant. The dotted line in Figure 15(c) is the boundary between the stable and unstable regions shown in Figure 14, and this indicate that a system with only the heat sink is slightly more unstable that a system with hex.

Summary of Corrigendum

In our recent IJSCD article titled ''Passive control of instabilities in combustion systems with heat exchanger'', we erroneously used the *sectional* (pertaining to the cross-sectional area in Fig. 3) heat absorption rate instead of *global* (pertaining to the total cross-sectional area) rate for the calculation of the 'heat sink coefficient' (α). This error resulted in the neglecting of α in the parametric study and in the subsequent stability analysis, provided in the article. The revised and rectified analysis provides the following results:

- We observe that the unstable mode of the combustor can be passively controlled to a large extent by varying the mean flow velocity $\bar{u}$ and the cavity length l_c.
- For the rigid downstream end condition ($R_p = 1$), an increase in cavity length favoured stability.
- Even though, frequency cannot be treated as a parameter, the variation in heat source location (l_f) manifested as a variation in the eigenfrequencies in the stability maps i.e., as l_f decreased, the $\omega_1 = \Re(_1)$ increased, and this favours stability.
- For an already unstable mode of the combustor, a decrease in mean velocity is shown to stabilise it.
- The stability maps constructed for the heat sink (alone) shows that stability decreases with increasing $\bar{u}$, while the stability maps for the tube row (alone) shows that the stability increases with increasing $\bar{u}$. The stability

maps constructed for the hex show that the net influence of the hex on the stability of the combustion system modelled is a combined effect of the heat losses at the heat sink as well as the acoustic losses at the tube row due to vortex dissipation. In our analysis, the heat sink was seen to dominate and hence for the system with hex, the stability decreases with increasing $\bar{u}$.

References

10. A. P. Dowling, and I. J. Hughes, Sound absorption by a screen with a regular array of slits, Journal of Sound and Vibration, 156 (1992), 387–405.